

# One-Shot Underwater 3D Reconstruction

Miquel Massot-Campos, Gabriel Oliver-Codina

Departament de Matemàtiques i Informàtica, Universitat de les Illes Balears

Cra. Valldemossa, km. 7,5 07122 Palma de Mallorca (Spain)

Email: {miquel.massot,goliver}@uib.es

**Abstract**—A one-shot sensor for underwater 3D reconstruction is presented and tested underwater in a water tank. The system is composed of a RGB CCD camera and a 532 nm green laser with a Diffractive Optical Element attached to it. The laser projects a pattern of parallel lines into the scene. The deformed pattern obtained in the camera frame is then processed to obtain a non-dense 3D point cloud that can be later used for autonomous manipulation and grasping, or for detailed mapping of textureless objects or scenarios.

## I. INTRODUCTION

Detailed spatial data is a requirement for diverse robotic applications like mapping or autonomous grasping. For example, a manipulator must know which object is facing and where the possible grasp points are prior to the intervention.

In underwater environments there is the added difficulty of the medium. 3D data acquisition is usually done using either sonar or an optical sensor. The latter is more common as it is cheaper than its counterpart, and much lighter and small.

Optical performance in underwater environments is strongly related to the water absorption and scattering coefficients, which depend on the turbidity and the amount of suspended particles in the media. This performance can be enhanced by choosing the light source wavelength to match the optimal underwater wavelength that minimizes both absorption and scattering. Consequently, if a laser light is also chosen, polarization filters can be also used to discard the light scattered by suspended particles.

## II. RELATED WORK

Different underwater 3D sensors available nowadays are mainly based on stereoscopy, time of flight light or triangulation, either from a projector or a laser source. In [1] a good overview of the different technologies is provided, but in underwater environments the next examples have been found:

In [2] and [3] stereoscopy is used to perform 3D reconstructions with bottom looking camera pairs. Textureless environments are hard to map only with image descriptors and matching. 3D reconstruction can also be obtained with a single camera using Structure from Motion [4].

In [5], two cameras and a structured light (SL) projector are tested in different water conditions to outperform stereoscopy. One camera and a SL projector have been used as well [6]. In the first case the projected light is used in the stereo matching as an extra texture, whilst in the second, 3D information is obtained knowing the calibration of the projector and triangulating the light rays coming from the camera and the

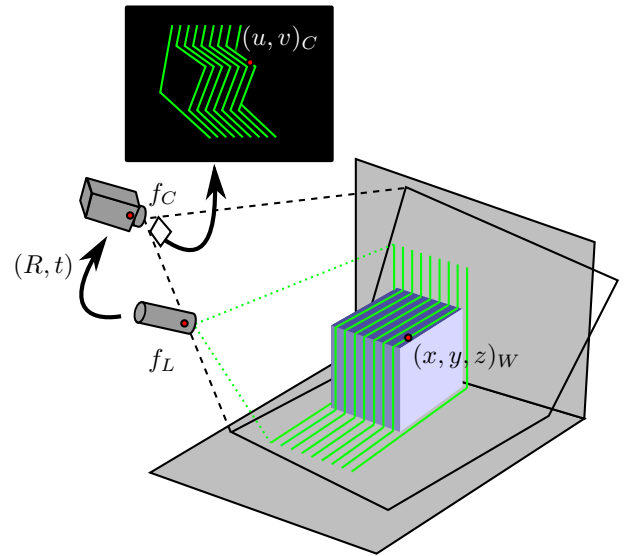


Figure 1. Basis of triangulation. The laser pattern is projected on an object, which deforms the pattern. This deformed lines are recovered by the camera. Laser focal point is  $f_L$  and camera focal point is  $f_C$ . Point  $(u, v)_C$  is the projections of point  $(x, y, z)_W$  from world coordinates to camera coordinates.  $(R, t)$  is the transformation matrix from the laser to the camera.

projector itself. However, SL suffers from needing a large amount of light that, in underwater environments, can result in a large amount of scattered light.

Laser light can solve that problem. A narrower beam can be directed to the target, reducing scattering problems. For that reason, slits are widely used to survey an area prior to manipulation [7], even with two cameras to avoid singularities or unseen slit parts [8]. Slits can be also created using light projectors [9]. Although slower, these systems provide a better accuracy and a good rejection of scattered light. The movement of the slit can be done with a manipulator or moving the vehicle while scanning. Depending on the accuracy of the pose of the vehicle, the latter may not be suitable for detailed 3D reconstructions.

Time of flight sensors using laser are also used, but require the vehicle to be stationary or to deploy the sensor [10]. Modulation techniques have been also used to reject scattered light [11]. These sensors are able to measure further distances and with a high precision, but require a sweep time to perform a measurement.

One shot 3D reconstruction has been proved in air [12] [13] with good results, and underwater robotics can benefit from

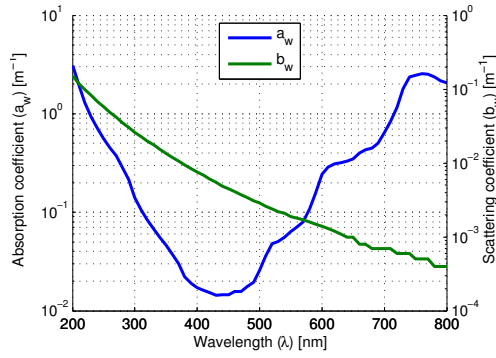


Figure 2. Absorption and scattering coefficients in pure seawater. Reproduced from Smith and Baker (1981).

it.

A one-shot underwater sensor capable of 3D reconstruction can provide enough data in one frame to an autonomous manipulator so it can grasp an object, regardless of the condition of the autonomous robot, either if it is stationary, slowly drifting, or approaching a target.

The system presented in this paper is capable of providing a non-dense point cloud in one camera shot, using a projection pattern and a triangulation method between the sensed pattern in the camera frame and the calibration knowledge.

This article is structured as follows: the description of the sensor is given in section III, the experimental setup in IV, the results in section V and the conclusions in section VI.

### III. DESIGN AND IMPLEMENTATION

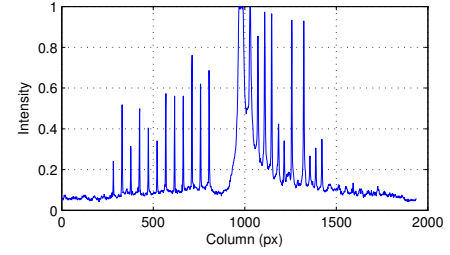
The sensor presented in this paper is formed by a camera and a green laser. In front of the laser source, a Diffractive Optical Element (DOE) has been placed to modify the beam shape to a set of parallel lines. These lines are projected on the scene and recovered by the camera. In Fig. 1 a schematic of the system is shown.

The laser lines have to be detected in the camera image, its peaks extracted and matched to their corresponding source laser line. Once the relation between a peak pixel and the laser plane is known, the 3D information can be computed by triangulation.

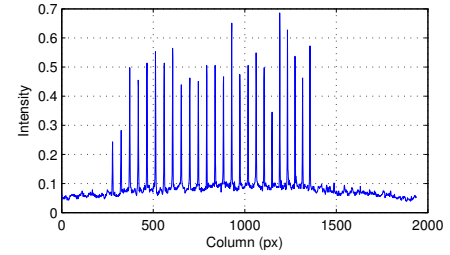
A 532 nm laser has been chosen as light source, as color is extremely important in underwater environments due to absorption and scattering. Those coefficients vary depending on the wavelength of the light source, as depicted in Fig. 2. In order to transmit the maximum light they have to remain low. Blue-green color spectra present a good compromise between absorption and scattering.

#### A. Geometric calibration

The camera has been modelled as a pinhole camera with a determined projection matrix. This matrix has been obtained by previous underwater camera calibration using a checkerboard pattern (e.g. calibration pattern), taking into account the housing port as well as the camera optics. Therefore the



(a) Central dot row.



(b) Other rows.

Figure 3. Intensity values of the rows in the image. Note the saturated value at the central dot.

camera intrinsic parameters are known. White balance has to be also calibrated with a white target beforehand.

The laser source can be modelled as a projector, e.g. inverse camera, with a particular camera matrix containing its focal distances and center distances. However, with the method presented in this paper, there is no need to calculate those parameters. Only the geometric transformation between the camera and the laser is needed. This transformation is extremely important, as all the results depend on the correctness of this calibration. Once this step is done, there is no need to redo it again unless the placement of the laser respect to the camera changes (for a different baseline, different working distance).

The calibration is performed by projecting the laser on a known plane at different distances, saving all the 3D points for fitting planes afterwards.

1) *Plane fitting*: Plane fitting calibration is performed by registering all 3D line points and matching them to their corresponding laser planes. In order to do that, a set of images at different depths are captured, projecting the laser on a flat surface with a checkerboard pattern on it.

The calibration pattern is captured by the camera and, knowing the size of each cell of the checkerboard, the plane equation can be obtained.

Then the laser is detected in the images and ray traced to the corresponding calibration plane. This step is done in every captured frame. After each line has been detected in all images, every line point belonging to the same laser plane is used to fit a 3D plane using a least square approach.

The coefficients of those planes are then saved for a posterior triangulation.

### B. Image processing pipeline

The process to obtain 3D information from a frame is split in four steps: acquisition, segmentation, decoding and triangulation.

1) *Acquisition*: The acquisition process is an important part where illumination and/or color changes have to be checked. The exposure of the camera has to be set so that the only saturated pixels in the image are the ones belonging to the central laser dot, to capture the gaussian pattern of the lines. Therefore, a peak detector can be used on these peaks to achieve better accuracy (see figure 3).

2) *Segmentation*: First, the background illumination has to be removed in order to be able to process the lines. For that, the red channel is subtracted to the green channel. Then each row is convolved with a median filter, and the result is removed from the original signal. Therefore, the median filter is used as a low pass filter to normalize the intensity in the image, without altering the laser lines. Finally, a binary image is computed by simple thresholding of the previous result, and the line centres are found for each row of the image.

For each center, the neighbouring values at the original image are checked, and the peaks are found using the center of mass method [14]. The centres that do not reach a certain intensity value are also discarded. Other authors have used the first, or even the second derivative to compute those peaks [15].

3) *Decoding*: It is difficult to determine which captured stripe corresponds to which projected stripe, when we attempt to index the captured sequence in the same order as the projected sequence. This is called the *correspondence problem*.

The output image of the segmentation stage is scanned row by row for rows where all the lines are indexable. Once those are identified and labelled, a flood fill algorithm [16] is used to propagate those indexes through all the detections.

4) *Triangulation*: With the labelling and the calibration, each 3D point  $p(t)$  can be computed by triangulating its corresponding laser plane  $\pi_n$  to the line formed by joining the segmented pixel to the camera focal point, which depends on the scale factor  $t$ .

$$\pi_n : Ax + By + Cz + D = 0 \quad (1)$$

$$p(t) = \left( \frac{u - c_x}{f_x} t, \frac{v - c_y}{f_y} t, t \right) \quad (2)$$

$$t = \frac{-D}{A \frac{u - c_x}{f_x} + B \frac{v - c_y}{f_y} + C} \quad (3)$$

where  $(f_x, f_y)$  is the camera focal length in  $x$  and  $y$  axes.  $(c_x, c_y)$  is the central pixel in the image.  $(u, v)$  is the detected laser peak pixel in the image.

Replacing 3 in 2, the 3D coordinates of the point are obtained.

### IV. EXPERIMENTAL SETUP

The camera used in the experiments is a Manta G-283C from Allied Vision Technologies with a 12 mm optics, an

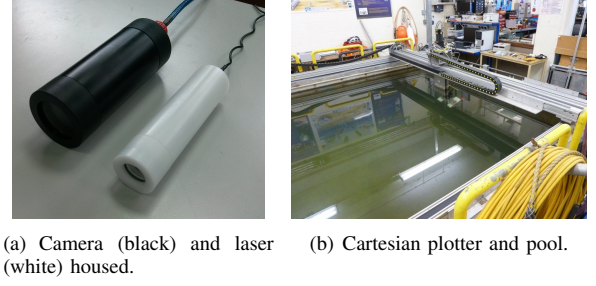


Figure 4. Experimental setup held at OSL-HWU.

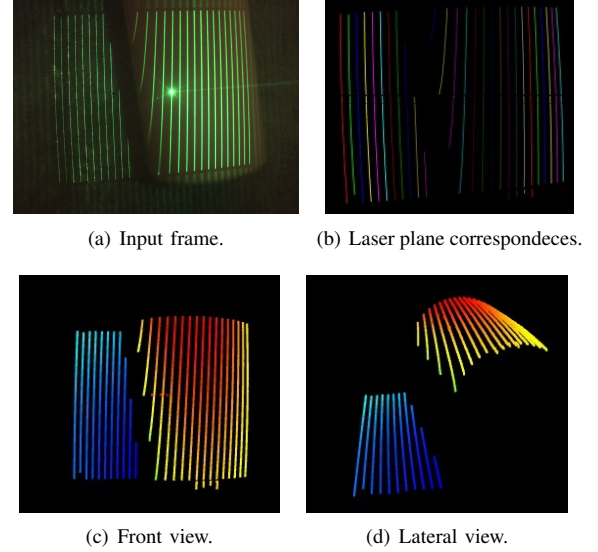


Figure 5. 3D reconstruction of a pipe.

CCD camera with  $1936 \times 1458$  pixels running at a maximum of 30 *fps*, depending on the exposure setting. The camera is interfaced to a Linux PC running ROS through an Ethernet port.

The laser is a 5 mW ZM-18B green laser from Z-Laser. The projected pattern is formed by 25 parallel lines, inscribed in a perfect square with a field of view of  $21^\circ$  in air,  $17^\circ$  in water. The pattern also has a brighter dot in the center of the square, due to the direct transmission of the original laser beam through the DOE.

These two components have been placed with an approximate baseline of 20 cm, aiming the laser  $10^\circ$  closer to the director vector of the camera.

In Fig. 4(a) the real system is shown unmounted, and in Fig. 4(b), it is shown mounted in a pool on a cartesian robot to perform the experiments. These two housings have been designed to be mounted on an Autonomous Underwater Vehicle (AUV) for future experiments.

### V. RESULTS

Previous to the design presented here, different options were modelled and tested on a simulator [17].

The calibration of the system has been made with eight different frames, taken from different view angles and dis-

tances to the checkerboard plane. The output of the calibration has confirmed the angle between laser light planes to be  $0.6875^\circ \approx 17^\circ/25$ .

Two reconstruction experiments have been carried out. In the first one, a 16 cm diameter textureless plastic pipe, Fig. 5(a), and in the second, a 15 cm plastic weight plate, Fig. 6(a).

In both experiments, the correspondence output from the decoding stage can be seen, correspondingly, in Fig. 5(b) and 6(b), where each line has been drawn in a different color. In the rows near the area where the central beam hits the target can be seen that the scattering and the light reflectance produces small inconsistencies in the correspondence solving.

Both reconstructions closely reproduce the original geometry. From the point cloud, the pipe roughly measures 13 cm width within the visible silhouette and the plate measures 14 cm in diameter.

## VI. CONCLUSION

This system has been capable of a one shot reconstruction. The output 3D data can be used to find objects or to match them to a known object database.

The correct detection of the laser depends on the contrast between the lines and the background, thus it may not work when ambient light is high. Even so, the system has been designed to operate under tenths of meters of water, where darkness is guaranteed.

The correspondence problem is still a issue to be solved, and there's still information available to help that solution. Correct tracking over time of the laser points could be fed into a filter or a processor to enhance the correct and to increase the point cloud density.

Future work includes extensive testing in a pool and in the ocean with different turbidity levels, and improvements of the correspondence algorithm.

Other DOEs are also in the scope of this study. More lines or different patterns could be used, even from different lasers to provide a wider field of view.

## ACKNOWLEDGMENT

The authors would like to thank Oceans System Laboratory, in Heriot-Watt University (OSL-HWU) for their facilities and support in the experiments. This work has been partially supported by the Ministry of Education of Spain (FPI grant BES-2012-054352).

## REFERENCES

- [1] F. Blais, "Review of 20 years of range sensor development," *Journal of Electronic Imaging*, vol. 13, no. 1, p. 231, 2004.
- [2] C. Beall, B. J. Lawrence, V. Ila, and F. Dellaert, "3D reconstruction of underwater structures," in *2010 IEEE/RSJ International Conference on Intelligent Robots and Systems*, vol. 0448111. IEEE, Oct. 2010, pp. 4418–4423.
- [3] T. D. Dao, "Underwater 3D reconstruction from stereo images," Msc Erasmus Mundus in Vision and Robotics, University of Girona (Spain), University of Burgundy (France), Heriot Watt University (UK), 2008.
- [4] O. Pizarro, R. M. Eustice, and H. Singh, "Large Area 3-D Reconstructions From Underwater Optical Surveys," *IEEE Journal of Oceanic Engineering*, vol. 34, pp. 150–169, 2009.

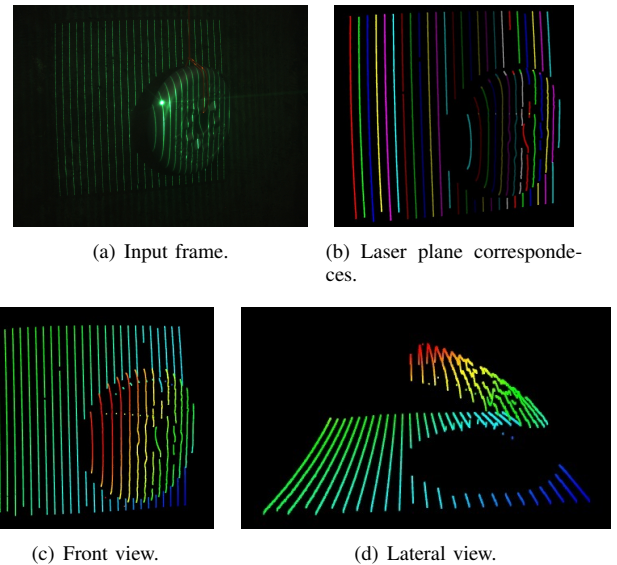


Figure 6. 3D reconstruction of a 1 kg plate.

- [5] F. Bruno, G. Bianco, M. Muzzupappa, S. Barone, and A. Rationale, "Experimentation of structured light and stereo vision for underwater 3D reconstruction," *ISPRS Journal of Photogrammetry and Remote Sensing*, vol. 66, no. 4, pp. 508–518, Jul. 2011.
- [6] N. Törnblom, "Underwater 3D Surface Scanning using Structured Light," Ph.D. dissertation, Uppsala Universitet, 2010.
- [7] M. Prats, J. J. Fernandez, and P. J. Sanz, "An approach for semi-autonomous recovery of unknown objects in underwater environments," in *2012 13th International Conference on Optimization of Electrical and Electronic Equipment (OPTIM)*. IEEE, May 2012, pp. 1452–1457.
- [8] E. P. n. González, F. S.-T. Díaz-Pache, L. P. Mosquera, and J. P. Agudo, "Bidimensional measurement of an underwater sediment surface using a 3D-Scanner," *Optics & Laser Technology*, vol. 39, no. 3, pp. 481–489, Apr. 2007.
- [9] S. Narasimhan and S. Nayar, "Structured Light Methods for Underwater Imaging: Light Stripe Scanning and Photometric Stereo," in *Proceedings of OCEANS 2005 MTS/IEEE*. Ieee, 2005, pp. 1–8.
- [10] F. R. Dalgleish, F. M. Caimi, W. B. Britton, and C. F. Andren, "Improved LLS imaging performance in scattering-dominant waters," in *Proc. SPIE*, W. W. Hou, Ed., vol. 7317, May 2009, pp. 73 170E–73 170E–12.
- [11] L. J. Mullen, V. M. Contarino, A. Laux, B. M. Concannon, J. P. Davis, M. P. Strand, B. W. Coles, and M. Contarion, "Modulated laser line scanner for enhanced underwater imaging," in *SPIE Proceedings*, G. D. Gilbert, Ed., vol. 3761. SPIE, Oct. 1999, pp. 2–9.
- [12] H. Kawasaki, R. Furukawa, R. Sagawa, and Y. Yagi, "Dynamic scene shape reconstruction using a single structured light pattern," *2008 IEEE Conference on Computer Vision and Pattern Recognition*, pp. 1–8, Jun. 2008.
- [13] K. Iwasaki, K. Terabayashi, and K. Umeda, "Construction of a compact range image sensor using a multi-slit laser projector suitable for a robot hand," *2012 IEEE/RSJ International Conference on Intelligent Robots and Systems*, pp. 4517–4523, Oct. 2012.
- [14] R. Fisher and D. Naidu, "A comparison of algorithms for subpixel peak detection," *Image Technology, Advances in Image Processing, Multimedia and Machine Vision*, 1996.
- [15] J. Forest Collado, J. Salvi, and E. Cabruja, "Laser stripe peak detector for 3D scanners. A FIR filter approach," in *Proceedings of the 17th International Conference on Pattern Recognition (ICPR'04)*, 2004, pp. 2–5.
- [16] A. Robinson, L. Alboul, and M. Rodrigues, "Methods for indexing stripes in uncoded structured light scanning systems," *WSCG*, vol. 12, no. 1, 2004.
- [17] M. Massot Campos and G. Oliver Codina, "Evaluation of a laser based structured light system for 3D reconstruction of underwater environments," in *Martech 2013 5th International Workshop on Marine Technology*. Girona: SARTI, 2013.